Eur. Phys. J. A (2017) **53**: 27
DOI 10.1140/epja/i2017-12213-x

THE EUROPEAN PHYSICAL JOURNAL A

Regular Article – Experimental Physics

Study of the β^- decay of ^{116m1}In: A new interpretation of low-lying 0^+ states in ^{116}Sn

J.L. Pore[1,a], D.S. Cross[1], C. Andreoiu[1], R. Ashley[1], G.C. Ball[2], P.C. Bender[2,b], A.S. Chester[1], A. Diaz Varela[3], G.A. Demand[3], R. Dunlop[3], A.B. Garnsworthy[2], P.E. Garrett[3], G. Hackman[2], B. Hadinia[3], B. Jigmeddorj[3], A.T. Laffoley[3], A. Liblong[3], R. Kanungo[4], B. Noakes[1], C.M. Petrache[5], M.M. Rajabali[2,c], K. Starosta[1], C.E. Svensson[3], P.J. Voss[1,d], Z.M. Wang[1,2], J.L. Wood[6], and S.W. Yates[7]

[1] Department of Chemistry, Simon Fraser University, 8888 University Drive, Burnaby BC, V5A 1S6, Canada
[2] TRIUMF, 4004 Wesbrook Mall, Vancouver BC, V6T 2A3, Canada
[3] Department of Physics, University of Guelph, 50 Stone Road, Guelph ON, N1G 2W1, Canada
[4] Department of Astronomy and Physics, Saint Mary's University, 923 Robie Street, Halifax NS, B3H 3C3, Canada
[5] CSNSM, CNRS-IN2P3, Universite Paris-Saclay, 91405 Orsay Cedex, France
[6] School of Physics, Georgia Institute of Technology, 837 State Street, Atlanta GA, 30332-0430, USA
[7] Departments of Chemistry and Physics & Astronomy, University of Kentucky, Lexington KY, 40506-0055, USA

Received: 6 December 2016 / Revised: 16 January 2017
Published online: 16 February 2017 –
Communicated by A. Jokinen

Abstract. The ^{116}Sn nucleus contains a collective rotational band originating from proton π $2p$-$2h$ excitations across the proton $Z = 50$ shell gap. Even though this nucleus has been extensively investigated in the past, there was still missing information on the low-energy interband transitions connecting the intruder and normal structures. The low-lying structure of ^{116}Sn was investigated through a high-statistics study of the β^- decay of ^{116m1}In with the 8π spectrometer and its ancillary detectors at TRIUMF. These measurements are critical in order to properly characterize the π $2p$-$2h$ rotational band. Weak γ-decay branches are observed utilizing γ-γ coincidence spectroscopy methods, leading to the first direct observation of the 85 keV $2_2^+ \rightarrow 0_3^+$ γ ray with a transition strength of $B(E2) = 99.7(84)$ W.u. The analysis of these results strongly suggests that the 2027 keV 0_3^+ state should replace the previously assigned 1757 keV 0_2^+ state as the band-head of the π $2p$-$2h$ rotational band.

1 Introduction

The tin isotopes have played a major role in understanding the structure of singly closed shell nuclei. The ^{116}Sn nucleus, in particular, stands out as one of the best-studied examples [1]. However, a less well-recognized aspect of ^{116}Sn is that it is also one of the best examples accessible for a detailed spectroscopic study of intruder states [2].

A major challenge to the exploration of intruder states in ^{116}Sn, and indeed in all of the tin isotopes, is that often the electromagnetic transitions that carry the critical information about shape coexistence are difficult to measure. There has been a lack of sensitivity for observing these low-energy transitions in γ-ray spectroscopy due to the phase space energy factor associated with electromagnetic decay (E_γ^5 for $E2$ transitions), which means that little or no information is available for non-yrast intruder states and for the transitions that reveal information on the mixing between different structures. (For a recent illustration of the elucidation of a shape coexisting structure by the discovery of a weak high-lying γ ray see ref. [3].)

A partial level scheme of the low-lying states in ^{116}Sn is presented in fig. 1, while table 1 contains all spectroscopic information obtained in this work. The level scheme includes the low-spin members of the quasi-rotational band that originates from π $2p$-$2h$ excitations. There is much that can be inferred about the structure of these states from previous measurements.

The 0_2^+ and 0_3^+ states: The 1757 keV 0_2^+ state has been previously assigned as the band-head of the π $2p$-$2h$ rotational band due to the strong population of a state at 1.84 MeV in two-proton transfer reactions [4]. However, it should be noted that due to the poor energy resolution of the measurement ($\sim$ 600 keV), the possibility that

[a] *Present address*: LBNL, 1 Cyclotron Road, Berkeley, CA 94720, USA; e-mail: jpore@lbl.gov
[b] *Present address*: NSCL, 640 S Shaw Ln, East Lansing MI, 48824, USA.
[c] *Present address*: Department of Physics, Tennessee Technological University, Cookeville, TN 38505, USA.
[d] *Present address*: Department of Physics, Concordia College, Moorhead, MN 56562, USA.

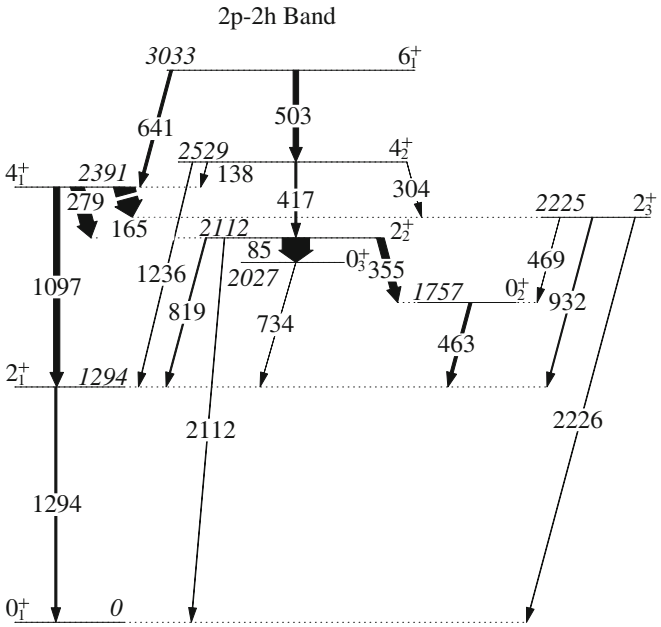

Fig. 1. A partial level scheme of ^{116}Sn where only selected transitions are presented to highlight the strong mixing that occurs between the low-spin members of the intruder band with other low-lying states. The widths of the arrows represent the $E2$ transition strengths. Only lower limits are available for the 138, 304 and 417 keV transitions, and an upper limit has been placed on the 165 keV transition. The half-life of the 3033 keV state has not been measured, so the widths of the arrows for the 503 and 641 keV γ rays represent their $B(E2)$ values relative to each other. The 3033 keV 6_1^+ state was not populated in the decay of the 5^+ ^{116m1}In isomer, its branching ratios are taken from ref. [5].

both the 0_2^+ and 0_3^+ states were populated in the reaction cannot be ruled out. These 0^+ states are connected by a strong $E0$ transition ($\rho^2 E(0) \cdot 10^3 = 87(19)$ [6]), which indicates strong mixing that has been investigated further with detailed studies of the $B(E2)$ transition probabilities [7]. The 2^+ rotational band member (at 2112 keV) populates the 0_2^+ the 0_3^+ states via 355 and 85 keV γ rays, respectively. The intensity of the 85 keV γ ray has not been directly measured, but an estimate of the ratio $B(E2; 85\,\text{keV})/B(E2; 355\,\text{keV})$ has been reported as 1.3(5) [8]. This suggests the band-head properties may be equally shared between the two exited 0^+ states, and makes it unclear which state should be considered the head of the rotational band. This result should be treated with some caution as it is dependent on an estimate of the intensity of the 85 keV γ ray and γ-ray intensities from ref. [9]. Even though questions were raised as to which 0^+ state was the band-head of the π $2p$-$2h$ band [10], the 1757 keV 0_2^+ state was adopted.

The 2_2^+ and 2_3^+ states: There is no evidence that suggests strong mixing between these low-lying 2^+ states. As only weak transitions are observed populating the excited 0^+ states from the 2225 keV 2_3^+ state, the majority of the rotational character of the π $2p$-$2h$ band is assumed to be contained in the 2112 keV 2_2^+ state. The 2225 keV 2_3^+ state is strongly populated in the (d, p) reaction with a spectroscopic factor of 0.98 [11], indicating a predominant neutron character. The different configurations of these two states are further highlighted by the absence of the 113 keV γ ray that would connect them.

The 4_1^+ and 4_2^+ states: The 2391 keV 4_1^+ and 2529 keV 4_2^+ states are both populated by the 6^+ member of the rotational band (at 3033 keV) via 641 keV and 503 keV γ rays, respectively. The half-life of the 3033 keV state has not been measured, but the ratio $B(E2; 641\,\text{keV})/B(E2; 503\,\text{keV})$ can be deduced as 1.9(2) from previously reported γ-ray branching ratios [12]. Each 4^+ state has a strong transition strength to the 2^+ rotational band member (at 2112 keV), which suggests that these states both contain π $2p$-$2h$ character. Further evidence of the similar structure of these states comes from the observation of the 138 keV γ ray that connects them. This fact suggest that the 4_1^+ and 4_2^+ states are mixed in a similar manner to the 0_2^+ and 0_3^+ states.

The low-lying levels of ^{116}Sn are populated in the β^- decay of ^{116}In. In the past, such studies have been limited; there are measurements from over 30 years ago [7, 10], and a recent study constrained to γ-ray singles spectroscopy [13]. Today, intense sources of mass-separated radioactive indium isotopes can readily be produced, and when combined with large arrays of Compton-suppressed high-purity germanium (HPGe) detectors, allow for very weak decay branches in the tin daughters to be studied with high precision.

In the present work the nature of these low-lying states is further investigated in a detailed study of ^{116}Sn from a high-statistics β^- decay measurement. Evidence is presented to show that the 2027 keV 0_3^+ state should replace the 1757 keV 0_2^+ state as the band-head of the intruder π $2p$-$2h$ rotational band.

2 Experimental setup

The measurements were performed with the 8π spectrometer at the TRIUMF-ISAC facility in Vancouver, BC [14]. A radioactive beam of ^{116}In was produced by spallation reactions of a 70 μA, 500 MeV proton beam delivered by the TRIUMF cyclotron onto a ^{nat}Ta high-power production target. A singly charged mass-separated beam of $A = 116$ ions was produced with a surface ionization source. The resulting beam delivered to the 8π spectrometer consisted of $1.2 \times 10^4\,\text{s}^{-1}$ of the $I^\pi = 1^+$ $T_{1/2} = 14.10(3)$ s ^{116g}In ground state, $4.0 \times 10^6\,\text{s}^{-1}$ of the $I^\pi = 5^+$ $T_{1/2} = 54.29(17)$ min ^{116m1}In isomer, and $3.2 \times 10^5\,\text{s}^{-1}$ of the $I^\pi = 8^-$ $T_{1/2} = 2.18(4)$ s ^{116m2}In isomer.

The beam was implanted onto a moveable Mylar tape at the center of the 8π spectrometer for cycles of one hour of beam implantation followed by one hour without beam. The implantation spot on the tape was transported behind a thick lead wall after each cycle to reduce the probability of detection of any long-lived contaminants that may have been present. The 8π spectrometer consists of 20

Table 1. Populated levels in ^{116}Sn from the β^- decay of ^{116m1}In. The $B(E2)$ values in Weisskopf units (W.u.) are given as determined from this analysis. Where necessary, the mixing ratio δ (taken from ref. [5]) was used to determine the $B(E2)$ value. Previously reported I_γ values [13] and $B(E2)$ values [5] are shown for comparison.

E_{level} (keV)	$T_{1/2}$ ref. [5]	$J_i^\pi \to J_f^\pi$	E_γ (keV)	I_γ	BR_γ	$B(E2)$ (W.u.)	I_γ ref. [13]	$B(E2)$ ref. [5]
1293.76(20)	0.374(10) ps	$2_1^+ \to 0_1^+$	1293.651(84)	100	100	12.4(3)	100	12.4(4)
1756.80(14)	44(6) ps	$0_2^+ \to 2_1^+$	463.244(23)	0.824(21)	100	18(2)	0.855(10)	18(3)
2026.91(65)	160(20) ps	$0_3^+ \to 2_1^+$	733.65(90)	0.00369(13)	100	0.49(7)		0.49(7)
2112.19(14)	1.89(10) ps	$2_2^+ \to 0_3^+$	85.294(88)	0.00166(10)	0.0091(6)	99.7(84)		
		$2_2^+ \to 0_2^+$	355.432(18)	0.939(23)	5.16(14)	44.4(28)	0.861(10)	44(5)
		$2_2^+ \to 2_1^+$	818.546(41)	14.2(3)	78.2(19)	7.8(7)	14.3(1)	7.7(8)
		$2_2^+ \to 0_1^+$	2112.346(90)	18.2(2)	100	0.115(6)	17.8(2)	0.118(7)
2225.37(16)	2.4(12) ps	$2_3^+ \to 0_2^+$	468.41(15)	0.000868(87)	0.75(9)	1.5(8)		1.0(6)
		$2_3^+ \to 2_1^+$	931.394(47)	0.116(6)	100	5.2(27)	0.106(5)	5(3)
		$2_3^+ \to 0_1^+$	2225.28(11)	0.0584(7)	50.2(27)	0.042(21)	0.055(2)	0.05(3)
2266.22(15)	0.34(4) ps	$3_1^- \to 2_1^+$	972.743(14)	0.631(16)	100		0.585(6)	
		$3_1^- \to 0_1^+$	2266.21(11)	0.00138(14)	0.211(23)		0.0036(6)	
2366.10(17)	348(19) ns	$5_1^- \to 3_1^-$	99.815(13)	0.0304(9)	84.1(29)	1.29(10)	0.028(3)	2.46(16)
		$5_1^- \to 2_1^+$	1071.53(9)	0.0348(16)	100			
2390.80(14)	0.47(9) ps	$4_1^+ \to 3_1^-$	124.634(24)	0.0140(5)	0.0203(7)		0.012(2)	
		$4_1^+ \to 2_3^+$	165.43(21)	< 0.013	< 0.019	< 66	0.016(2)	
		$4_1^+ \to 2_2^+$	278.850(14)	0.158(5)	0.228(9)	49(10)	0.154(10)	60(10)[a]
		$4_1^+ \to 2_1^+$	1096.761(55)	69.2(8)	100	22.5(43)	69.0(7)	23(5)[a]
2529.40(14)	< 100 ps	$4_2^+ \to 4_1^+$	138.252(7)	4.63(11)	13.7(5)	> 0.6[b]	4.63(10)	
		$4_2^+ \to 5_1^-$	163.300(51)	0.0242(9)	0.0719(35)		0.018(2)	
		$4_2^+ \to 3_1^-$	263.271(14)	0.160(4)	0.476(19)		0.148(5)	
		$4_2^+ \to 2_3^+$	304.017(15)	0.142(3)	0.420(15)	> 0.23	0.142(7)	> 0.23
		$4_2^+ \to 2_2^+$	417.001(21)	33.7(10)	100	> 11.2	32.1(3)	> 12
		$4_2^+ \to 2_1^+$	1235.838(90)	0.0683(36)	0.203(12)	$> 9.97 \times 10^{-5}$	0.006(3)	> 0.00017
2650.42(33)		$2_4^+ \to 2_1^+$	1356.10(13)	0.00471(37)	100		0.0093(13)	
		$2_4^+ \to 0_1^+$	2650.34(21)	0.000609(6)	12.9(16)			
2773.01(40)		$6_1^- \to 5_1^-$	406.860(63)	0.0150(7)	100			
2801.28(15)		$4_3^+ \to 4_2^+$	272.203(15)	0.0404(13)	0.344(14)		0.045(4)	
		$4_3^+ \to 4_1^+$	409.901(36)	0.0735(26)	0.627(27)		0.071(3)	
		$4_3^+ \to 5_1^-$	434.573(37)	0.0288(11)	0.245(11)		0.027(3)	
		$4_3^+ \to 3_1^-$	535.016(31)	0.0405(13)	0.345(14)		0.040(3)	
		$4_3^+ \to 2_2^+$	688.737(35)	0.209(7)	1.78(8)		0.196(4)	
		$4_3^+ \to 2_1^+$	1507.123(94)	11.7(3)	100		11.7(1)	
2908.48(41)	0.5(3) ns	$7_1^- \to 6_1^-$	135.460(15)	0.00996(30)	62.3(34)			
		$7_1^- \to 5_1^-$	542.461(84)	0.160(7)	100		0.40(24)	
2996.05(38)		$3_1^+ \to 4_4^+$	194.74(10)	0.00191(26)	14.8(31)			
		$3_1^+ \to 4_2^+$	468(1)	0.00305(42)	23.6(49)			
		$3_1^+ \to 4_1^+$	604(1)	0.00285(43)	22.1(48)			
		$3_1^+ \to 2_3^+$	771(1)	0.00554(11)	43.0(67)			
		$3_1^+ \to 2_1^+$	1702.06(14)	0.0129(20)	100			
3045.90(18)		$4_4^+ \to 4_3^+$	244.685(24)	0.0360(12)	1.29(5)		0.039(3)	
		$4_4^+ \to 2_4^+$	395.190(50)	0.00620(33)	0.222(13)		0.0080(25)	
		$4_4^+ \to 4_2^+$	516.06(16)	0.0189(18)	0.679(68)		0.015(2)	
		$4_4^+ \to 4_1^+$	655.046(30)	0.141(4)	5.05(20)		0.145(3)	
		$4_4^+ \to 5_1^-$	679.892(41)	0.0246(11)	0.883(44)		0.025(6)	
		$4_4^+ \to 3_1^-$	779.656(39)	0.301(8)	10.8(4)		0.291(5)	
		$4_4^+ \to 2_1^+$	1752.12(10)	2.79(7)	100		2.78(3)	
3096.67(19)		$4_5^+ \to 3_1^+$	100.49(7)	0.0229(17)	1.23(10)			
		$4_5^+ \to 4_3^+$	295.47(9)	0.00750(66)	4.02(37)			
		$4_5^+ \to 2_4^+$	447.08(10)	0.00153(15)	0.818(85)			
		$4_5^+ \to 4_2^+$	567.510(30)	0.0522(21)	28.0(14)		0.064(5)	
		$4_5^+ \to 4_1^+$	705.743(36)	0.187(5)	100		0.189(3)	
		$4_5^+ \to 3_1^-$	829.83(47)	0.0443(14)	23.8(10)		0.034(6)	
		$4_5^+ \to 2_3^+$	870.53(13)	0.00609(44)	3.26(25)			
		$4_5^+ \to 2_1^+$	1802.83(51)	< 0.00545	< 3.00		0.0105(20)	
3209.17(49)		$7_2^- \to 6_1^-$	436.153(37)	0.00184(11)	71(10)			
		$7_2^- \to 5_1^-$	843.96(50)	0.00259(32)	100		> 0.054	

[a] Values taken from ref. [7].
[b] Determined with $\delta = -0.13^{+0.09}_{-0.13}$ value from ref. [16].

high-purity germanium (HPGe) detectors equipped with bismuth germanate (BGO) Compton-suppression shields. The array was coupled with a plastic scintillator for β particle detection, located at zero degrees with respect to the beam, and the PACES array of 5 Si(Li) detectors for conversion-electron detection [15]. The resultant γ-singles data contained 6×10^9 events. The γ-γ coincidences were sorted into a time-random-background–subtracted matrix that contained 4×10^8 events. Calibration data were taken with sources of ^{56}Co, ^{60}Co, ^{133}Ba, and ^{152}Eu. Presently the results of the γ-ray analysis will be discussed, the results of the conversion-electron analysis are presented in ref. [16].

3 Analysis

Branching ratios were determined from the analysis of the γ-γ coincidence data by gating either from above or from below the γ ray of interest. Gating from below is advantageous for the observation of weak γ rays, such that the intensities can be determined by the method developed by Kulp *et al.* [17] utilizing

$$N_{12} = N I_{\gamma 1} \epsilon(\gamma_1) B_{\gamma 2} \epsilon(\gamma_2) \epsilon_{12} \eta(\theta_{12}), \quad (1)$$

where N_{12} is the number of counts in a coincidence peak between two cascading γ rays, N is the overall normalization factor that characterizes the specific decay data set, $I_{\gamma 1}$ is the intensity of the "feeding" γ ray (γ_1), $B_{\gamma 2}$ is the branching ratio of γ_2 relative to all (γ and conversion-electron) intensity depopulating the same excited state, $\epsilon(\gamma_1)$ and $\epsilon(\gamma_2)$ are the singles photopeak efficiencies, ϵ_{12} is the coincidence efficiency, and $\eta(\theta_{12})$ is the angular correlation factor.

4 Results

For the purposes of this work, only the beam-off data were analyzed to insure that the low-lying levels in ^{116}Sn were only populated by the $T_{1/2} = 54.29(17)$ min 5^+ ^{116m1}In state and not from the short-lived ($T_{1/2} = 14.10(3)$ s) 1^+ ^{116g}In ground state. The observed intensities, branching ratios, and $E2$ transition probabilities for the γ rays relevant for this discussion are presented in table 1. Note that the 3033 keV 6_1^+ state was not populated in this data set.

In the present work, fifty-seven γ-ray transitions were identified, four of which have not previously been observed. The observed energies, relative intensities, γ-branching ratios (BR_γ), and $B(E2)$ transition strengths for levels with previously reported lifetimes [5] for the transitions are reported in table 1. The values for BR_γ are reported as the intensity of each γ ray relative to the most intense γ ray depopulating the same excited state. The γ-ray intensities from the most recent publication of the β^- decay of ^{116m1}In by Krane and Sylvester [13] and previously reported $B(E2)$ values [5] are also listed in table 1 for comparison. Intensities were observed down to $6.09(6) \times 10^{-4}$% of the $2_1^+ \rightarrow 0_1^+$ ground-state 1294 keV transition. The reported level energies were determined from a global-χ^2 minimization of the observed γ-ray energies. The results are in good agreement with what has been previously reported.

Table 2. Observed β feeding for levels in ^{116}Sn populated by the decay of ^{116m1}In. The $\log ft$ values were calculated with ref. [19] and previously reported β-feeding percentages from ref. [13] are shown for comparison.

E_{level} (keV)	J_i^π	β (%)	$\log ft$	β (%) ref. [13]
2391	4^+	53.1(9)	5.19(9)	54.2(6)
2529	4^+	33.6(9)	5.16(14)	32.5(3)
2801	4^+	10.2(3)	5.10(15)	10.3(1)
2908	7^-	0.0241(6)	7.43(11)	
3046	4^+	2.79(7)	4.90(19)	2.82(4)
3097	4^+	0.26(1)	5.72(3)	0.24(3)
3209	7^-	0.0039(3)	6.9(3)	

The intensity balances for each level were examined so that the β feeding could be deduced; missing intensity from conversion electrons was taken into account with theoretical conversion coefficients determined from BrIccFO calculations [18]. In addition to the previously reported allowed β transitions, two first-forbidden β transitions are present populating the 7^- 2908 and 3209 keV levels that have not been previously observed. The deduced β feedings into levels of ^{116}Sn are shown in table 2 compared to the previously reported values from Krane and Sylvester [13] alongside calculated $\log ft$ values [19].

The first direct observation of the $2_2^+ \rightarrow 0_3^+$ 85 keV γ ray was obtained by gating on the 734 keV $0_3^+ \rightarrow 2_1^+$ γ ray (fig. 2(a)). Previous works only report an estimate of this intensity [8]. From the current work the 85 keV transition is found to have a relative intensity of 0.00166(10), which translates into a $B(E2)$ transition strength of 99.7(84) Weisskopf units (W.u.), calculated as per ref. [20]. Investigations of the Compton-scatter background that surrounds the 734 keV peak show that none of the observed intensity of the 85 keV peak in the 734 keV gate is due to Compton-scatter events of the 819 keV γ ray (see fig. 2(b), (c)).

5 Discussion

Previously, the rotational character of the π $2p$-$2h$ bandhead was believed to be distributed between the 1757 keV 0_2^+ and 2027 keV 0_3^+ states due to the estimated ratio of $B(E2; 85\,\text{keV})/B(E2; 355\,\text{keV}) = 1.3(5)$ [8]. The similar strength of the 355 and 85 keV transitions from the 2_2^+ π $2p$-$2h$ state to the 0_2^+ and 0_3^+ levels, respectively, indicated a similar distribution of the intruder-rotational character to each 0^+ state. However, this interpretation was dependent on an estimation of the intensity of the 85 keV $2_2^+ \rightarrow 0_3^+$ γ ray.

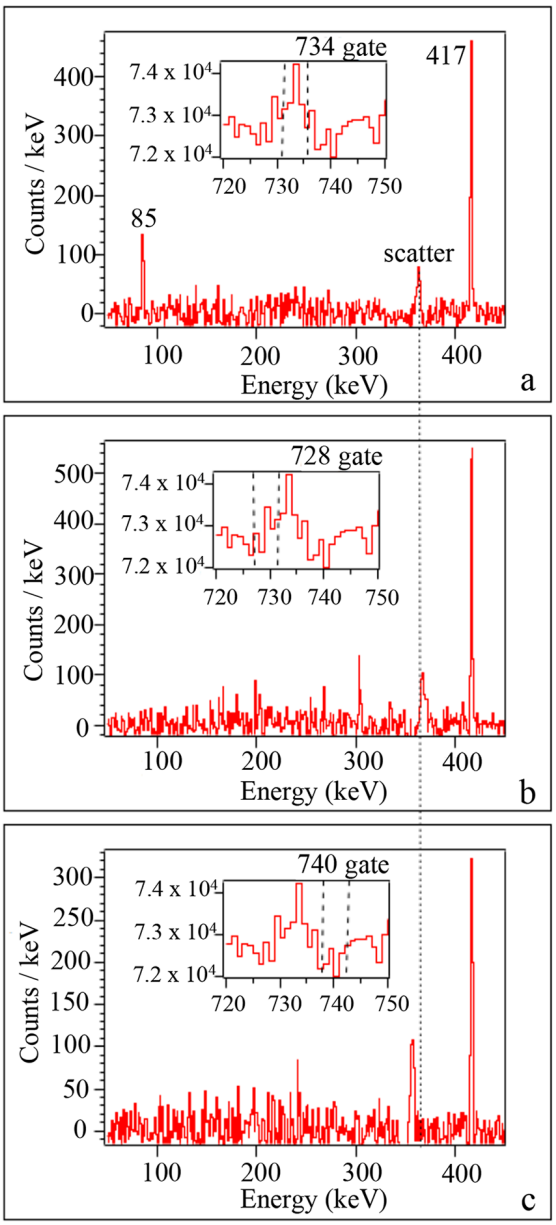

Fig. 2. The insets of each plot show the region of the γ-γ matrix that was gated to obtain each γ-ray spectrum. (a) The γ-ray energy spectrum obtained from gating on the random-background–subtracted γ-γ coincidence matrix from below on the 734 keV $0_3^+ \rightarrow 2_1^+$ γ ray to observe the weak 85 keV $2_2^+ \rightarrow 0_3^+$ gamma ray. The "scatter" feature is not from a real γ ray, but rather Compton-scatter events from the 1097 keV γ ray that are an artifact of the gate on the 734 keV γ ray. The width of this peak is equal to the width of the gate. To determine whether or not there were Compton-scatter events from the 819 keV γ ray in the 85 keV peak area gates were taken on either side of the 734 keV peak. The γ-ray spectrum obtained by gating between energies 727 and 731 keV and between energies 738 and 742 keV are shown in (b) and (c), respectively. Notice that the centroid of the scatter peak is different in each gate, and that there is no corresponding scatter peak in the region of the 85 keV peak in either (b) or (c). The gated region is dominated by Compton scatter from the 1294 keV γ ray, which accounts for the presence of the 417 keV peak in (b) and (c).

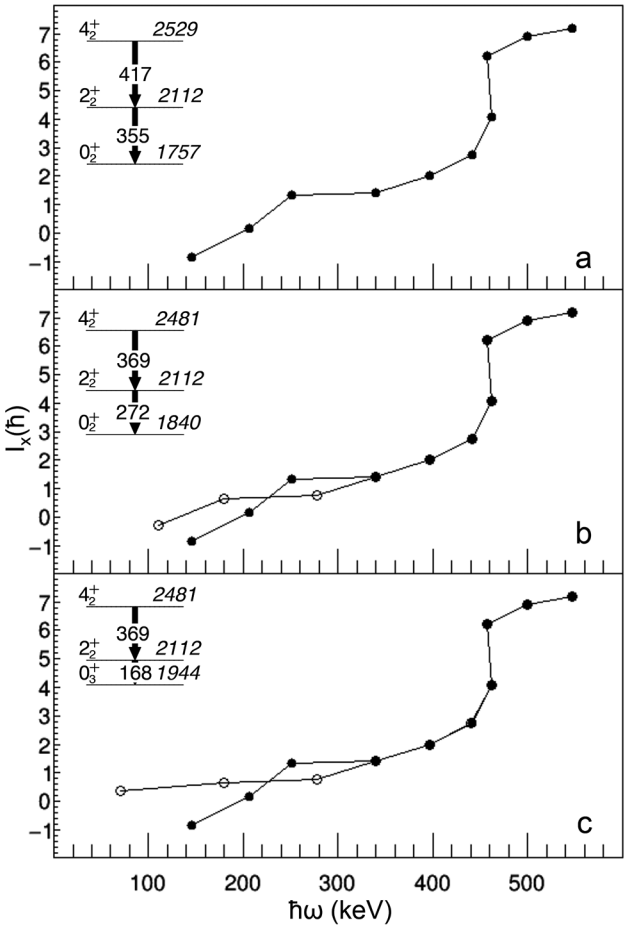

Fig. 3. Particle alignment plots for the ^{116}Sn intruder rotational band (up to spin 20^+ [21]): (a) with the observed experimental energies of the 0_2^+, 2_2^+, and 4_2^+ states; (b) with the substitution of the determined unperturbed energies of the 0_2^+ and 4_2^+ state overlapped with (a); (c) with the substitution of the 0_3^+ state as the band-head overlapped with (a). A comparison of the three plots clearly indicates that the 0_3^+ state is the more suitable band-head compared to the 0_2^+ state. The Harris parameters used here are $J_0 = 15\hbar^2\,\mathrm{MeV}^{-1}$ and $J_1 = 25\hbar^4\,\mathrm{MeV}^{-3}$ as were employed in ref. [21].

In the present work, the intensities of both the 355 and 85 keV γ rays have been determined directly. The ratio of the reduced transition probabilities $B(E2; 85\,\mathrm{keV})/B(E2; 355\,\mathrm{keV})$ is 2.2(3). The 2_2^+ π $2p$-$2h$ state populates the 0_3^+ state with twice the strength as it populates the 0_2^+ state. This strongly suggests that the 2027 keV 0_3^+ state should be the band-head of the π $2p$-$2h$ rotational band instead of the previously assigned 1757 keV 0_2^+ state.

To explore this possibility, the characteristics of the π $2p$-$2h$ intruder band have been further investigated. A look at the behavior of the aligned angular momenta of the intruder band with the observed experimental energies of the 0_2^+, 2_2^+, and 4_2^+ states shows a clear irregularity at low rotational frequencies below $\hbar\omega \sim 250$ keV (fig. 3(a)). Previously, this irregularity has been attributed to the strong mixing between the intruder and normal configu-

Table 3. Results of the two-state mixing calculation used to determined the unperturbed energies (E_{unp}) of the low-lying mixed pairs of 0^+ and 4^+ states. All energies are in units of keV.

J^π	E_{exp}	$R_{B(E2)}$	α^2	β^2	V (keV)	ΔE_S	E_{unp}
0_2^+	1757	2.2(3)	0.69	0.31	125	83	1840
0_3^+	2027						1944
4_1^+	2391	1.9(2)	0.65	0.35	66	48	2438
4_2^+	2529						2481

rations at low spin [21]. There is strong mixing of the low-lying 0^+ (0_2^+ and 0_3^+) and 4^+ (4_1^+ and 4_2^+) states, whereas there is little evidence to support strong mixing of the 2^+ (2_2^+ and 2_3^+) states.

If mixing were indeed the source of the perturbation present in the alignment plot at $\hbar\omega \sim 250$ keV, then it should be possible to restore a smooth behavior by analyzing the mixing of these states replacing the energies of the experimentally observed states with those of the unperturbed ideal states. To disentangle each pair of states a simple two-state mixing calculation was performed utilizing the measured ratio of $E2$ transition probabilities ($R_{B(E2)}$) populating each mixed state from the π $2p$-$2h$ rotational band. In this method, it is assumed that the wave function of the higher-lying (hl) and lower-lying (ll) states with a particular J^π can be written as a linear combination of pure intruder ($Intr.$) and normal ($Norm.$) states:

$$|hl\rangle = \alpha\,|Intr.\rangle + \beta\,|Norm.\rangle\,, \quad (2)$$

$$|ll\rangle = \beta\,|Intr.\rangle - \alpha\,|Norm.\rangle\,, \quad (3)$$

$$\alpha^2 + \beta^2 = 1. \quad (4)$$

Then, assuming β to be the smaller mixing amplitude, it is possible to extract the interaction strength V to determine the energy by which each experimentally observed state is shifted (ΔE_s) by the interaction, such that the unperturbed energy of each state (E_{unp}) can be determined. The results for the 0^+ and 4^+ states are presented in table 3. Note that a different interaction strength V is calculated for each pair of states, because it is assumed that the normal configuration present in the pair of 0^+ states is different than the normal structure contained in the pair of 4^+ states.

In an attempt to minimize the observed irregularity, one can redraw the alignment plot by substituting the experimental 0_2^+ and 4_2^+ energies with the unperturbed energies of 1840 and 2481 keV, respectively. However, the irregularity is still present at $\hbar\omega = 180$ keV as is seen in fig. 3(b). It is clear that this is due to the unperturbed energy of the 0_2^+ state, which is too low. If it is replaced with the unperturbed energy of 1944 keV corresponding to the 0_3^+ state, a smoother behavior is obtained at low spins (fig. 3(c)). This result, in addition to the newly measured $B(E2)$ value for the 85 keV gamma ray, clearly suggests the 2027 keV 0_3^+ state as the band-head of the intruder structure in ^{116}Sn.

Further evidence would come if the large $B(E2)$ of the 85 keV transition were observed to continue at higher angular momenta within the intruder structure. The half-life of the 2529 keV 4^+ intruder-band member has not been precisely measured (< 100 ps [7]), so there is currently only a lower-limit set on the $B(E2)$ of the 417 keV $4_2^+ \rightarrow 2_2^+$ transition of > 11 W.u. For the 417 keV transition to have a $B(E2) \sim 100$ W.u., similar to the $B(E2)$ of the 85 keV gamma ray, the half-life of the 2529 keV state would be on the order of 10 ps.

Currently, there is no obvious extension for the reinterpretation of the ^{116}Sn intruder band in the neighbouring even-even $^{114-120}$Sn isotopes due to a lack of information on γ-ray branching ratios. However, two low-lying excited 0^+ states, close in energy, have been observed in each of these isotopes [5]. Further investigation of these nuclei with the goal of detecting weak decay branches is necessary to properly characterize the collectivity in the tin region. Such a campaign is feasible with similar high-statistics β decay studies with high-efficiency spectrometers.

6 Conclusion

Based on new measurements of γ-ray branching ratios presented here, there is strong evidence to indicate that the 2027 keV 0_3^+ state is the band-head of the π $2p$-$2h$ rotational band in ^{116}Sn. Further experiments to measure the lifetime of the 4^+ band member could elucidate whether the large $B(E2)$ value observed for the 85 keV transition continues at higher angular momentum. For a transition of ~ 100 W.u., the half-life of the 4_2^+ state would be on the order of 10 ps.

The authors acknowledge the insightful discussions on shell model calculations in ^{116}Sn with Dr. Alfredo Poves. This work was supported in part by the Natural Sciences and Engineering Research Council (Canada). TRIUMF receives funding via a contribution agreement through the National Research Council (NRC) of Canada. This material is based upon work supported by the U.S. National Science Foundation under Grant No. PHY-1305801.

References

1. S. Raman *et al.*, Phys. Rev. C **43**, 521 (1991).
2. K. Heyde, J.L. Wood, Rev. Mod. Phys. **83**, 1467 (2011).
3. A. Chakraborty *et al.*, Phys. Rev. Lett. **110**, 022504 (2013).
4. H.W. Fielding *et al.*, Nucl. Phys. A **281**, 389 (1977).
5. J. Blachot, Nucl. Data Sheets **111**, 717 (2010).
6. T. Kibédi, Spear, At. Data Nucl. Data Tables **89**, 77 (2005).
7. J. Kantele *et al.*, Z. Phys. A **289**, 157 (1979).
8. N.-G. Jonsson, A. Bäcklin, R. Julin, J. Kantele, M. Migahed, Institute of Physics, University of Uppsala, UUIP-1000 report (1979).
9. D. Rabenstein, Z. Phys. **240**, 244 (1970).

10. A. Bäcklin *et al.*, Nucl. Phys. A **351**, 490 (1981).
11. E.J. Schneid *et al.*, Phys. Rev. **156**, 1316 (1966).
12. J. Bron *et al.*, Nucl. Phys. A **318**, 335 (1979).
13. K.S. Krane, J. Sylvester, Phys. Rev. C **73**, 54312 (2006).
14. A.B. Garnsworthy, P.E. Garrett, Hyperfine Interact. **225**, 122 (2014).
15. E.F. Zganjar *et al.*, Acta Phys. Pol. B **38**, 1179 (2007).
16. D.S. Cross *et al.*, in preparation.
17. W.D. Kulp *et al.*, Phys. Rev. C **76**, 34319 (2007).
18. T. Kibédi *et al.*, Nucl. Instrum. Methods Phys. Res. A **589**, 202 (2008).
19. NNDC logft calculator: `http://www.nndc.bnl.gov/logft/`.
20. R.B. Firestone, V.S. Shirley, *Table of Isotopes* (John Wiley & Sons, 1996).
21. A. Savelius *et al.*, Nucl. Phys. A **637**, 491 (1998).